Applied Surface Science 257 (2010) 1314–1318

Contents lists available at ScienceDirect

Applied Surface Science

journal homepage: www.elsevier.com/locate/apsusc

Integrity of functional self-assembled monolayers on hydrogen-terminated silicon-on-insulator wafers

Fangyuan Tian [a], Chaoying Ni [b], Andrew V. Teplyakov [a,*]

[a] Department of Chemistry and Biochemistry, University of Delaware, Newark, DE 19716, USA
[b] Department of Materials Science and Engineering, University of Delaware, Newark, DE 19716, USA

ARTICLE INFO

Article history:
Received 13 April 2010
Received in revised form 12 August 2010
Accepted 16 August 2010
Available online 20 August 2010

Keywords:
Silicon-on-insulator (SOI)
Self-assembled monolayers (SAMs)
Surface modification
X-ray photoelectron spectroscopy (XPS)
Transmission electron microscopy (TEM)

ABSTRACT

Silicon-on-insulator (SOI) wafers are commonly used to design microelectronics, energy conversion, and sensing devices. Thin solid films on the surfaces of SOI wafers have been a subject of numerous studies. However, SOI wafers modified by self-assembled monolayers (SAMs) that can also be used as functional device platforms have been investigated to a much lesser extent. In the present work, *tert*-butoxycarbonyl (*t*-boc, $(CH_3)_3$–C–O–C(=O)–)-protected 1-amino-10-undecene monolayers were covalently attached to a H-terminated SOI (1 0 0) surface. The modified wafers were characterized by X-ray photoelectron spectroscopy to confirm the stability of the SAM/Si interface and the integrity of the secondary amine in the SAM. The transmission electron microscopy investigation suggested that this *t*-boc-protected 1-amino-10-undecene SAM produces atomically flat interface with the 2 μm single crystalline silicon of the SOI wafer, that the SiO_x and both available Si/SiO_x interfaces are preserved, and that the organic monolayers are stable, with apparent thickness of 1.7 nm, which is consistent with the result of the density functional theory modeling of the molecular features within a SAM.

1. Introduction

The molecular-level control of surface modification and functionalization processes developed in recent years has already helped to convert a number of fundamental ideas into practical applications [1–3]. The fields that particularly benefited from these developments include catalysis, solar energy conversion, biosensing, and microelectronics. One of the particularly intriguing recent advances with a likely very high potential practical impact is the capabilities to produce highly controlled functional self-assembled monolayers (SAMs) on semiconductor substrates [1]. These layers can serve both as protective coatings against wear and chemical oxidation and as a functional starting point for further chemical modification of surfaces and interfaces. Strictly speaking, the nature of the monolayers produced by most common self-assembly of thiols on gold [4] is very different from the monolayers produced on semiconductor materials, such as, silicon, where the formation of a strong covalent bond between organic molecules [5] and the surface precludes these molecules from diffusing along the surface and "self-assemble". Nevertheless, since it is a commonly used terminology in semiconductor surface modification processing, we will refer to the monolayers produced on silicon as self-assembled monolayers (SAMs) as well.

While the dielectric properties of SAM can be tuned by altering the length and chemical nature of the molecular chain, the other attractive feature of the SAMs on silicon is a wide versatility of the functional surfaces produced. For example, amino-terminated ($-NH_2$) SAMs are frequently used for binding biological materials such as proteins and DNA, making these functional monolayers amenable for applications in biosensing and biomicroelectronics. A number of previous investigations of differently terminated SAMs, including $-CH_3$, –OH, and –COOH functionalities [6,7] on metals [8] and metal oxides [9], can serve as a reference point for the studies on silicon. In fact, silicon single crystals modified with various SAMs have also received very substantial attention and amino-terminated SAMs have been found to bind large molecules such as C_{60} fullerenes [10] and even DNA [11,12] and gold nanoparticles [13]. Amino-terminated organic molecules on silicon have also been investigated in structural characterization and even in organic reaction catalysis [14]. While the formation of SAMs on silicon single crystals and the attachment chemistry to the functional groups of these SAMs have been investigated substantially, the more practical platform for interfacing with common electronic devices, silicon-on-insulator wafers, and the integrity of SAMs on these wafers have rarely been a subject of a detailed investigation.

SOI wafer is composed of a film of single crystalline silicon (the device layer) separated by a layer of silicon oxide from the bulk silicon substrates (the handle layer). Within this structure, ionizing radiation and leakage currents are reduced remarkably, and power consumption by corresponding devices is greatly improved

* Corresponding author. Tel.: +1 302 831 1969; fax: +1 302 831 6335.
E-mail address: andrewt@udel.edu (A.V. Teplyakov).

0169-4332/$ – see front matter © 2010 Elsevier B.V. All rights reserved.
doi:10.1016/j.apsusc.2010.08.058

compared with conventional silicon wafer devices [15]. Therefore, within the past ten years, commercial applications of SOI have progressed exponentially.

SOI technology is usually interfaced into devices by applying selective ion implantation and metal deposition (for example, as a source and a drain for field effect-based applications [16]). That is why the behavior of thin solid films on SOI substrates is studied very commonly. However, much less research has been conducted showing modification of SOI by SAMs.

While it is expected that most of the chemistry developed for single crystalline silicon should hold true for the SOI wafers, it is also important to confirm this postulate experimentally, especially due to the fact that the structure and chemical reactivity of single crystalline silicon surfaces prepared by etching procedures are extremely sensitive to the specific preparation conditions. The Si–C bond has high bond strength (3.5 eV) [17] and low polarity, which makes it possible to covalently attach alkyl-based SAMs to silicon materials including SOI wafers. Since the $–NH_2$ termination is very susceptible to oxidation in ambient conditions, often the chemically protected functional groups are used at selected processing steps instead that can be easily converted back to $–NH_2$ functional layers. Here we will use the *t*-boc protected ($((CH_3)_3–C–O–C(=O)–$) 1-amino-10-undecene monolayers. The following questions should be answered to make the modification of SOI wafers with *t*-boc-protected amino-undecene universally applicable: (1) Can the SAM of *t*-boc-protected amino-undecene be formed on SOI wafers? (2) If the SAM is formed, is its chemical identity preserved (that is does the molecular structure of *t*-boc-protected amino-undecene remain stable after modification)? (3) Is the SAM/silicon interface created during SAM formation oxygen-free and is it stable? (4) Since the surface modification process involves preparation by wet etching and SAM formation at elevated temperatures up to 180–220 °C, does the buried silicon oxide layer maintain its integrity and stable Si/SiO_x interfaces?

In the present study, eleven-carbon chain *t*-boc-protected amino-terminated SAMs were attached to SOI (1 0 0) wafers. X-ray photoelectron spectroscopy (XPS) was used to investigate the integrity of the SAM formed and chemical identity of the molecules forming SAM, as well as to confirm that the SAM/Si interface is stable and essentially oxide-free. The transmission electron microscopy was employed to interrogate the structure of the SAM/Si interface, to confirm the integrity of the underlying SiO_x layer and both SiO_x/Si interfaces, and to deduce the apparent thickness of the SAM. Finally, the expected thickness of the SAM calculated with the help of density functional theory (DFT) modeling is compared with the experimental observation. It is generally important to obtain a visual characteristic of the SAM in addition to the spectroscopic identification of its integrity and this is also one of the goals of this work.

2. Experimental part

2.1. Materials

All chemicals were reagent grade or better and used as received: ammonium hydroxide (Fisher, 29% certified ACS plus grade), hydrochloric acid (Fisher, 37.3% certified ACS grade), hydrogen peroxide (Fisher, 30% certified ACS grade), buffer-HF improved (Transene Company, Inc.), trifluoroacetic acid (TFA) (Aldrich, 99%), methylene chloride (Fisher, 99.9%), petroleum ether (Fisher, certified ACS), methanol (Fisher, 99.9%), 1-chloro-10-undecene (Aldrich, 97%), potassium phthalimide (Fluka, ≥99.0%), hydrazine monohydrate (Fluka, ≥98.0%), dimethyl formamide (DMF) (Fisher, 99.8%), ethyl ether (Fisher, Laboratory Grade), ethanol (Pharmco, 99.5%), and toluene (Fisher, 99.9%). The deionized water used to rinse the surfaces and containers was from a first generation Milli-Q water system (Millipore) with 18 MΩ resistance.

The silicon-on-insulator (SOI) wafer was fabricated by Ultrasil Corporation. The device wafer was monocrystalline p-Si (boron doped, ⟨1 0 0⟩ orientation, 1–30 Ω cm, 2 ± 0.5 μm thick). The handle wafer was p-Si (boron doped, ⟨1 0 0⟩ orientation, 1–30 Ω cm, 625 ± 25 μm thick). The buried-oxide (BOX) thickness was 500 nm, according to the specifications.

2.2. Experimental details: sample preparation

2.2.1. Preparation of hydrogen-terminated SOI (1 0 0)

The hydrogen-terminated SOI (1 0 0) surface was prepared using standard modified RCA cleaning procedure [10] that is more commonly used for single crystalline (1 1 1) silicon wafers. This approach proved to be the most efficient. All reactions were carried out in Teflon beakers. The detailed steps of preparing hydrogen-terminated SOI (1 0 0) surface are as follows. The Teflon beakers and tweezers were cleaned in SC1 solution composed of 4:1:1 Milli-Q water, hydrogen peroxide, and ammonium hydroxide for 1 h on an 80 °C water bath with N_2 bubbler and rinsed with Milli-Q water. After being blown dry with N_2, the wafer was placed in the beaker and cleaned in SC1 solution for 10 min on an 80 °C water bath. Then, the wafer was rinsed with Milli-Q water several times, etched in HF buffer solution for 2 min and rinsed with Milli-Q water again. After that, the wafer was placed in the beaker filled with SC2 solution composed of 4:1:1 Milli-Q water, hydrogen peroxide, and hydrochloric acid for 10 min in an 80 °C water bath to grow a SiO_2 layer. Then, the rinsed wafer was etched in HF buffer solution for 1 min followed by 6 min of etching in ammonia fluoride solution to form hydrogen-terminated SOI (1 0 0) surface.

2.2.2. Preparation of self-assembled monolayers (SAMs) on SOI (1 0 0)

t-boc-protected 1-amino-10-undecene was synthesized by standard organic methods [10,18]. 5 ml *t*-boc protected 1-amino-10-undecene was placed in a 25 ml flask with a reflux condenser and kept under flowing N_2. The solution was deoxygenated with dry N_2 for at least 1 h. Subsequently, the hydrogen-terminated SOI (1 0 0) wafer was placed in the flask. Then, the flask was immersed in an oil bath, and the solution was refluxed for 2 h with a slow N_2 flow. After that, the SOI sample was removed from the solution and cleaned in petroleum ether (40–60 °C), methanol, and dichloromethane. The surface was then rinsed with Milli-Q water and dried with N_2.

2.3. Experimental details: characterization techniques

2.3.1. X-ray photoelectron spectroscopy (XPS)

The XPS spectra were collected on PerkinElmer ESCA 5500 with monochromatic Al Kα X-ray source. Before XPS analysis, the modified SOI (1 0 0) sample was evacuated in the introduction chamber for 24 h to remove volatile compounds present on the surface. The measurements were performed in a vacuum chamber with base pressure of 2×10^{-8} Torr. The X-ray power was 400 W. The data analysis was performed using Casa software.

2.3.2. Transmission electron microscopy (TEM)

TEM cross-section specimens were prepared by Helios NanoLab 600, a dual-beam focused ion beam and field emission scanning electron microscope. TEM images were collected with an objective lens C_s corrector Titan operating at 300 kV.

2.4. Computational details

Density functional theory (DFT) calculations were performed using the B3LYP/LANL2DZ approach [19–20] tested previously in

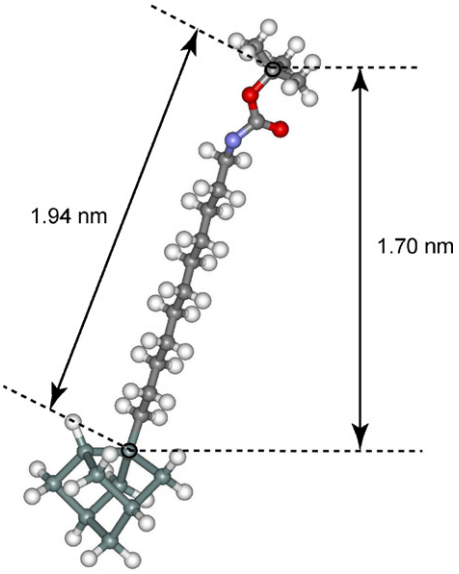

Scheme 1. *t*-boc-protected 1-amino-10-undecene reacted with an H-terminated Si_9H_{12} cluster representing the silicon–silicon dimer site on a SOI (1 0 0) surface predicted computationally at the B3LTP/LANL2DZ level of theory. The calculated length between the carbon atom (highlighted with black circle, top) of the *t*-boc group connected to oxygen and the silicon atom (highlighted with black circle, bottom) connected to alkyl chain was 1.94 nm. The calculated tilt angle was 19.9°.

our group [21–23], as implemented in the Gaussian 03 suite of programs [24]. The top device layer Si(1 0 0) was represented by a Si_9H_{12} cluster, shown in Scheme 1 reacted with *t*-boc protected 1-amino-10-undecene molecule and the opposite silicon site of the representative silicon dimer of the 2×1 reconstructed (1 0 0) surface saturated with a hydrogen atom. All the other silicon atoms were terminated by hydrogen to maintain their hybridization and all the atoms of the entire structure were allowed to relax upon energy minimization calculations. Energy minimization calculation was performed to estimate the thickness of the *t*-boc amino-terminated SAM. N 1s and C 1s core-level energies in the models were predicted using Koopmans' theorem, and the correction factor to the predicted core-level energy for N 1s was found to be 8.5 eV based on our previous investigations [25]. All of the predicted N 1s energies from calculations in this work were corrected by this factor and then were compared to the XPS experimental results.

3. Results and discussion

3.1. X-ray photoelectron spectroscopy investigation

The *t*-boc protected 1-amino-10-undecene SAM on the SOI (1 0 0) surface was investigated by XPS. C 1s, N 1s and Si 2p XPS spectra are presented in Fig. 1. The computationally predicted N 1s core-level energies of the model in Scheme 1 were calibrated for comparison with the experimental data as described in Section 2.4. The predicted values for C 1s are provided as the best alignment with experimental data. In Fig. 1a, the C 1s XPS spectrum of the *t*-boc protected 1-amino-10-undecene SAM exhibits a main feature at 284.6 eV and at least two more features that can be fitted at 286.8 and 289.0 eV. Computational predictions, which help to assign these peaks, are indicated by arrows in Fig. 1a and solid bars corresponding to the transitions themselves. The peak at 284.6 eV encompasses signature transitions corresponding to methyl groups of the *t*-boc entity and to the methylene groups of the alkyl chain except for the carbon atom connected to nitrogen. The peak at 286.8 eV combines information on the carbon atom connected to nitrogen and a carbon atom of the *t*-boc group connected to oxygen [10,26,27]. Finally, the feature at 289.0 eV corresponds to the carbon atom of the carboxylic group [10,26]. The intensity ratio corresponding to these peaks is consistent with the 1:2:11 ratio expected for this SAM; however, in the experimental data the intensity of the 284.6 eV feature is slightly higher than expected, which can be explained by adsorption of the adventitious carbon during sample transfer. The single observed N 1s XPS peak at 400.1 eV is assigned to the secondary amine group –NH– in the *t*-boc protected

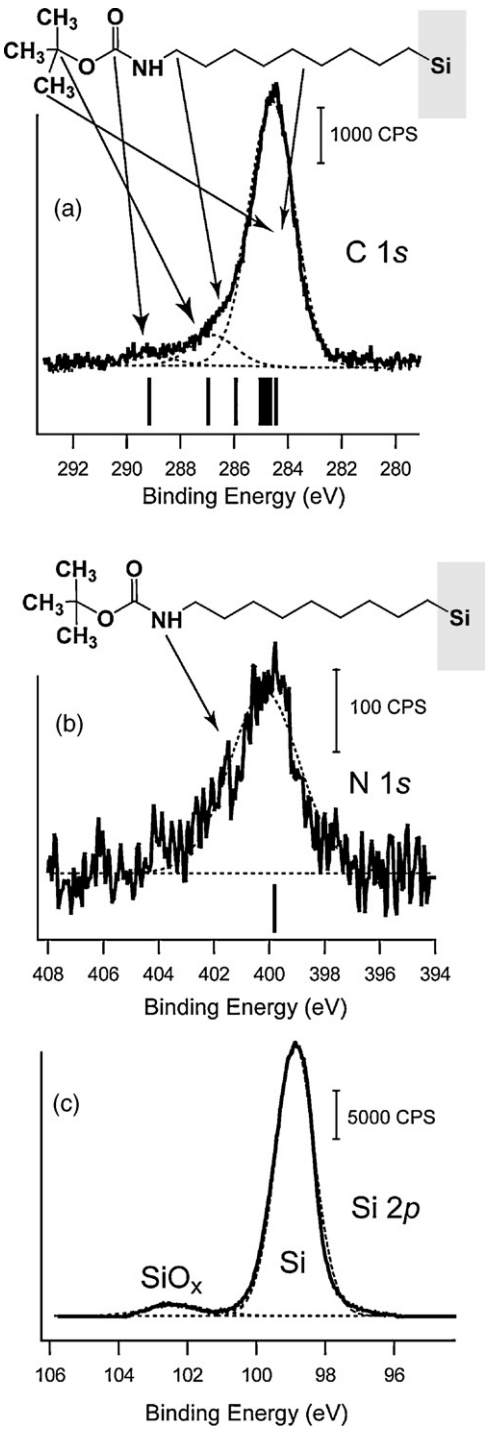

Fig. 1. XPS spectra of the SOI (1 0 0) surface: (a) C 1s for the *t*-boc 1-amino-10-undecene SAM on SOI (1 0 0); (b) N 1s for the *t*-boc 1-amino-10-undecene SAM on SOI (1 0 0); (c) Si 2p for the *t*-boc 1-amino-10-undecene SAM on SOI (1 0 0); (a) and (b) sections also compare the experimental XPS spectra for C 1s and N 1s with the core-level energy predicted for the model in Scheme 1, the computational results are shown as vertical solid bars.

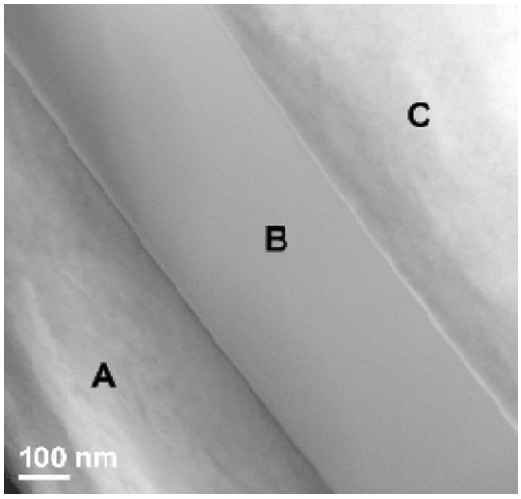

Fig. 2. Cross-sectional low resolution TEM image of SOI (1 0 0) wafer, which was modified by *t*-boc protected amino-terminated SAM, composed of Si(1 0 0) device layer (A), buried silicon oxide (B), and Si(1 0 0) substrate (C). After being modified by SAM, the buried silicon oxide layer remained intact.

1-amino-10-undecene SAMs, as shown in Fig. 1b, on the basis of the experimental data consistent with our computational prediction. It should be pointed out that the position of the N 1s peak indicates the integrity of the protected functional group, as this energy would change substantially if a primary amine was present or if functional group oxidation would take place [25]. Our previous studies found the binding energy corresponding to secondary amino group was at 397.2 [10] and 398.4 eV [29] for –NH– near less electrophilic functional groups. In our case, the *t*-boc group next to –NH– results in the shift of the observed N 1s peak to higher binding energy. Supplementary information presents a side-by-side comparison of the C 1s and N 1s XPS spectra for this SAM on SOI wafer used in this work and on a single crystalline Si(1 0 0) surface. Since these spectra are nearly identical, the chemical integrity of *tert*-butoxycarbonyl-protected 1-amino-10-undecene monolayers covalently attached to both surfaces is confirmed. In a spectrum shown in Fig. 1c, Si 2p region, the peak at 98.9 eV corresponds to silicon, while the small feature observed at 102.4 eV is due to partial surface oxidation [28]. The low intensity of the peak at 102.4 eV proves that the surface of SOI (1 0 0) wafer is stabilized with SAMs and is resistant with respect to ambient oxidation within the timeframe required to perform these experiments. Based on these XPS results, we estimate that the SiO_x corresponds to less than 6.5% of the monolayer.

3.2. Transmission electron microscopy studies

The structure of the *t*-boc 1-amino-10-undecene SAMs on SOI (1 0 0) substrates was investigated by both low and high-resolution cross-sectional TEM. From the low resolution micrograph presented in Fig. 2, the SOI layer-by-layer structure, composed of silicon substrates, buried silicon oxide, and the top silicon device layer is clearly recognizable. In addition, the thickness of the buried silicon oxide was measured to be 0.5 μm, consistent with the sample specifications.

The high-resolution micrograph of the very top surface shows the SAM layer with an apparent height of 1.7 nm, as shown in Fig. 3 at the top. Comparing this layer with the TEM images of amorphous silicon oxide [30,31], it can be deduced that the characteristics of these two materials in TEM experiments are different, consistent with the modification procedure confirmed by XPS, supporting the absence of surface oxidation in this sample. In addition, the observed thickness of the surface layer observed by TEM is consistent with the expected thickness of *t*-boc protected amino-terminated SAM.

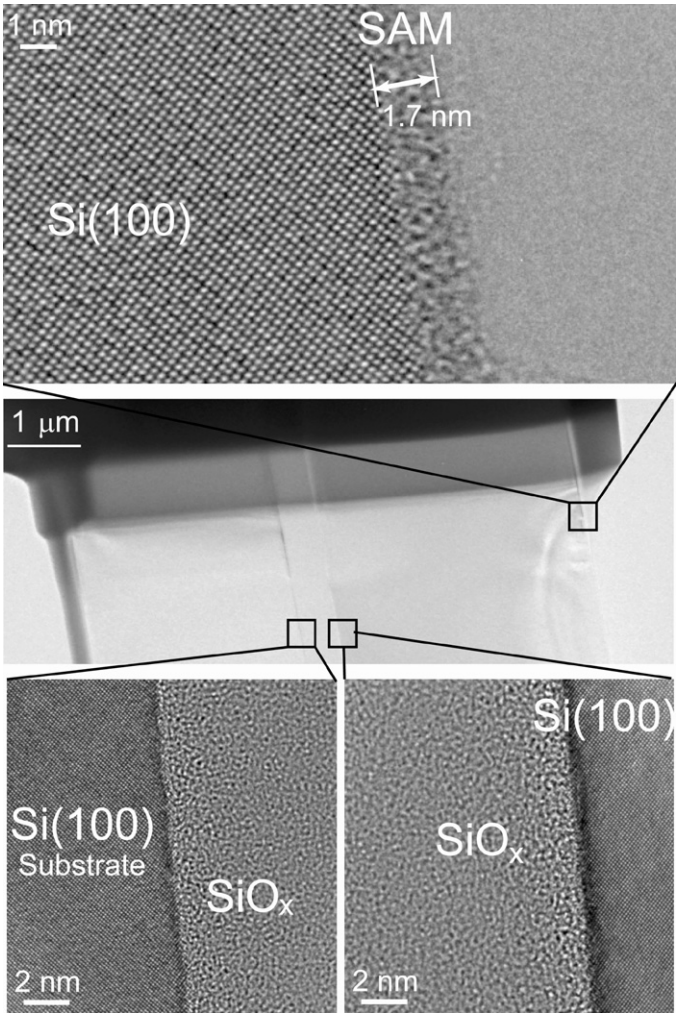

Fig. 3. Cross-sectional high-resolution TEM images of *t*-boc protected amino-terminated SAM on the Si(1 0 0) device layer (top), with apparent height of 1.7 nm. The interface region between buried silicon oxide and Si(1 0 0) substrate (bottom, left). The interface region between buried silicon oxide and Si(1 0 0) device layer (bottom, right). In the middle is another low resolution micrograph of the cross-section of *t*-boc protected amino-terminated SAM on SOI (1 0 0). Additional micrographs provided as Supplementary information illustrate the presence of the carbon deposited by the ion beam during focused ion beam sample preparation.

In the computational investigation summarized in Scheme 1, the length of alkyl *t*-boc 1-amino-10-undecene chain was estimated to be 1.94 nm, and the thickness of the SAM based on the individual molecule is expected to be approximately 1.7 nm, which is in excellent agreement with the TEM observations. Although the realistic tilt angles may deviate from the one predicted here computationally on Si(1 0 0) surface, the literature yields similar tilt angles for primary amino-terminated C_{12} alkyl monolayers on Si(1 1 1) surface [32–34]. Some deviations are expected for the predicted models as compared to the experimental observations but it is still remarkably consistent with the TEM studies presented above.

Two high-resolution micrographs presented in the bottom panels of Fig. 3 show the interfaces between the buried silicon oxide and device layer or handle layer. From these micrographs, it is clear that these interfaces remain intact following SOI (1 0 0) surface modification with SAM and sample preparation for TEM investigations.

4. Conclusions

In the present work, *t*-boc-protected 1-amino-10-undecene SAMs were covalently attached to the SOI (1 0 0) substrates. The analytical spectroscopic and microscopic methods were combined to understand the chemistry of this attachment. The N 1s XPS spectrum suggested the formation of a secondary amino group in the reaction of an amino-terminated SAM with H-terminated SOI (1 0 0) substrates, and the C 1s XPS confirmed that all the expected molecular features of the compound are present on the surface. The Si 2p XPS verified that the top thin film of silicon on SOI (1 0 0) wafer is nearly oxygen-free. Together with the computational investigation, the TEM studies evaluated the presence of the SAM on a surface of the SOI (1 0 0) wafer and the intactness of the buried silicon oxide layer, as well as the intactness of both Si/SiO_x interfaces.

Acknowledgments

This work was partially supported by the National Science Foundation (CHE-0650123). Acknowledgment is made to the Donors of the American Chemical Society Petroleum Research Fund for partial support of this research. We acknowledge the help of Dr. Sergei Rykov and the research group of Professor Jingguang Chen (Department of Chemical Engineering, University of Delaware) for their help with XPS measurements. Authors would like to thank FEI Company for the access to its NanoPort facility in Oregon for using the dual-beam equipment and the Titan TEM. Technical assistances from C. Bugge, B.V. Leer, Y.C. Wang, and L. Fu for sample preparation and data collection are greatly appreciated.

Appendix A. Supplementary data

Supplementary data associated with this article can be found, in the online version, at doi:10.1016/j.apsusc.2010.08.058.

References

[1] E. Ruckenstein, Z.F. Li, Adv. Colloid Interface Sci. 113 (2005) 43.
[2] P.K. Chu, J.Y. Chen, L.P. Wang, N. Huang, Mater. Sci. Eng. R 36 (2002) 143.
[3] S.F. Bent, Surf. Sci. 500 (2002) 879.
[4] J.C. Love, L.A. Estroff, J.K. Kriebel, R.G. Nuzzo, G.M. Whitesides, Chem. Rev. 105 (2005) 1103.
[5] F. Schreiber, Prog. Surf. Sci. 65 (2000) 151.
[6] R.G. Nuzzo, L.H. Dubois, D.L. Allara, J. Am. Chem. Soc. 112 (1990) 558.
[7] B. Fabre, F. Hauquier, J. Phys. Chem. B 110 (2006) 6848.
[8] V. Brunetti, B. Blum, R.C. Salvarezza, A.J. Arvia, Langmuir 19 (2003) 5336.
[9] R. Hofer, M. Textor, N.D. Spencer, Langmuir 17 (2001) 4014.
[10] X.C. Zhang, A.V. Teplyakov, Langmuir 24 (2008) 810.
[11] X.C. Zhang, S. Kumar, J.H. Chen, A.V. Teplyakov, Surf. Sci. 603 (2009) 2445.
[12] X.C. Zhang, I.H. Antonopoulos, S. Kumar, J.H. Chen, A.V. Teplyakov, Appl. Surf. Sci. 256 (2009) 815.
[13] J.W. Zheng, Z.H. Zhu, H.F. Chen, Langmuir 16 (2000) 4409.
[14] T. Bocking, M. James, H.G.L. Coster, T.C. Chilcott, K.D. Barrow, Langmuir 20 (2004) 9227.
[15] G.K. Celler, S. Cristoloveanu, J. Appl. Phys. 93 (2003) 4955.
[16] C.R. Newman, C.D. Frisbie, D.A.S. Filho, J.L. Bredas, P.C. Ewbank, K.R. Mann, Chem. Mater. 16 (2004) 4436.
[17] J.M. Buriak, Chem. Rev. 102 (2002) 1271.
[18] B.S. Alexander, R. Linke, G. Heij, G. Meijer, H. Zuilhof, E.J.R. Sudholter, Langmuir 17 (2001) 7554.
[19] A.D. Becke, J. Chem. Phys. 98 (1993) 5648.
[20] C. Lee, W. Yang, R.G. Parr, Phys. Rev. B 37 (1988) 785.
[21] L. Pirolli, A.V. Teplyakov, Surf. Sci. 600 (2006) 3313.
[22] L. Pirolli, A.V. Teplyakov, J. Phys. Chem. B 110 (2006) 4708.
[23] J.C.F. Rodríguez-Reyes, A.V. Teplyakov, J. Phys. Chem. C 111 (2007) 4800.
[24] M.J.T. Frisch, et al., Gaussian 03, Revision C.02, Gaussian, Inc., Wallingford CT, 2004.
[25] T.R. Leftwich, A.V. Teplyakov, J. Electron Spectrosc. Relat. Phenom. 175 (2009) 31.
[26] T. Strother, R.J. Hamers, L.M. Smith, Nucleic Acids Res. 28 (2000) 3535.
[27] A.A. Shestopalov, R.L. Clark, E.J. Toone, Langmuir 26 (2010) 1449.
[28] M.L. Yang, D. Wouters, M. Giesberst, U.S. Schubert, H. Zuilhof, ACS Nano 3 (2009) 2887.
[29] T.R. Leftwich, M.R. Madachik, A.V. Teplyakov, J. Am. Chem. Soc. 130 (2008) 16216.
[30] J. Cao, D. Pavlidis, Y. Park, J. Singh, A. Eisenbach, J. Appl. Phys. 83 (1998) 3829.
[31] A. Thogersen, J. Mayandi, T.G. Finstad, A. Olsen, J.S. Christensen, M. Mitome, Y. Bando, J. Appl. Phys. 104 (2008) 094315.
[32] S.L. Yuan, Y. Zhang, Y. Li, G.Y. Xu, Colloids Surf. A: Physicochem. Eng. Aspects 242 (2004) 129.
[33] C.S. Kwok, P.D. Mourad, L.A. Crum, B.D. Ratner, Biomacromolecules 1 (2000) 139.
[34] A. Bansal, X.L. Li, S.I. Yi, W.H. Weinberg, N.S. Lewis, J. Phys. Chem. B 105 (2001) 10266.